Earthquake Geotechnical Engineering for Protection and Development of Environment and Constructions – Silvestri & Moraci (Eds)
© 2019 Associazione Geotecnica Italiana, Rome, Italy, ISBN 978-0-367-14328-2

Effective stress analysis of liquefiable site in Christchurch to discern the characteristics of sediment ejecta

D. Hutabarat & J.D. Bray
University of California, Berkeley, USA

ABSTRACT: Dynamic effective stress analysis (ESA) is performed to back-analyze the seismic responses of a liquefiable site in Christchurch during the 2010-2011 Canterbury earthquake sequence. Different amounts of ejecta were observed at this site after earthquakes of different intensities and durations. The severity of liquefaction manifestations is used to assess the capability of ESA for estimating the likelihood and amount of ejecta. The ESA employs the PM4Sand and PM4Silt constitutive models after they were calibrated to capture the contractive-dilative response of liquefiable materials at the site. The simulation results show there is a unique trend between the computed excess pore water pressures and total head distributions to the severity of ejecta observed. The different patterns of the total head distribution generated by the earthquakes show promise as the basis for developing a methodology to estimate the amount of ejecta.

1 INTRODUCTION

The 2010-2011 Canterbury Earthquake Sequence (CES) produced numerous cases of buildings experiencing large differential settlement caused by sediment ejecta (e.g. Bray et al. 2014). Quantitative methods to estimate the amount of ejecta are not available. Early work examined the mechanisms producing liquefaction ejecta focusing on solutions of the diffusion equation (e.g. Housner 1958, Ambraseys & Sarma 1969). Later, empirical data were used by Ishihara (1985) to estimate the likelihood of ejecta occurring based on non-liquefiable crust thickness, liquefiable layer thickness, and peak ground acceleration (PGA) of earthquake shaking. His recommendations, however, are limited to sites with thick deposits of liquefiable clean sand. It does not address stratified soil sites. Moreover, it does not quantify the severity of the surface manifestation.

The amount of ejected sand at a site likely depends on the amount of excess pore water pressure that must be dissipated to reach steady-state condition. A free-field site at Shirley Intermediate School (Shirley) site in Christchurch, New Zealand is examined in this study to investigate the conditions leading to different amounts of ejecta during major events of the CES. The geological characteristics of the Shirley site are interpreted to enable one dimensional (1D) fully-coupled dynamic effective stress analyses (ESA) of the site using robust constitutive soil models that can capture pore water pressure generation and migration within the soil profile.

2 SITE DESCRIPTION

2.1 *Site, earthquakes, and surface manifestations*

The central and eastern areas of Christchurch are underlain predominantly by alluvial sands and silts. The depositional environment produced thick fine clean sand layers with increasing relative density at deeper elevations. The Shirley site (-43.510408, 172.661995) is a clean sand

Figure 1. Aerial photographs (source: New Zealand Geotechnical Database) of soccer field at Shirley site after major events of the 2010-2011 CES events. The yellow mark indicates areas covered by ejecta.

free-field site in the eastern quadrant of Christchurch. Figure 1 shows aerial photographs of the Shirley site several hours after shaken by the 2010 M_w 7.1 Darfield, 2011 February M_w 6.2 Christchurch, and 2011 M_w 5.6 and M_w 6.0 (separated by 80 minutes) June earthquakes. The classification of the manifestation is based on the total area covered by ejecta relative to the total area under assessment, which is within 20 m radius from SCPT-57366. The manifestation classification is divided into 5 categories: None, Minor, Moderate, Severe, and Extreme for 0%, 0-5%, 5-20%, 20-50%, and 50-100% covered area, respectively. A larger covered area indicates more severe surface manifestation that induces more ground subsidence due to ejecta. The computed median PGAs at the Shirley site using the Bradley (2013) ground motion model are 0.19 *g*, 0.38 *g*, and 0.25 *g* for the Darfield, Christchurch, and June earthquakes, respectively. These PGA values are similar to the recorded PGA values of 0.18 *g*, 0.33 *g* and 0.18 *g*, respectively, at the Shirley Library strong motion station (SHLC, -43.505, 172.6639), located 600 m to the north of the Shirley site.

2.2 *Subsurface conditions*

CPT and borehole data at the Shirley site are available from New Zealand Geotechnical Database (NZGD) website (*www.nzgd.org.nz*). The data from the closest points of the several CPTs at the site are presented in Figure 2. The dark and light red color background represents the Robertson (2009) normalized soil behavior type index (SBT_n, I_c) values of 1.31–1.8 and 1.8-2.05, which correspond to clean sand and silty sand mixtures at this site, respectively. The Shirley site is underlain by thick fine clean sand (> 15 m) with similar mean particle diameter. The CPT interpretation is supported by data from an adjacent borehole (BH-57258). The depth of the groundwater level (GWL) during the soil investigations and the earthquakes is approximately 2.0 m and 2.5 m, respectively.

The first layer is a 50-cm thick brown organic silt fill followed by non-plastic, yellowish brown sandy silt to silt until a depth of 3.5m. The soil above the groundwater table is categorized as a non-liquefiable layer for the CES events. The soil above a depth of 3.5 m has finer material and lower hydraulic conductivity than the underlying liquefiable clean sand soil so it will be modeled differently than the liquefiable soil layer. The layer below a depth of 3.5 m is the typical Christchurch Formation dark gray sand that forms a uniformly graded, very fine to fine, alluvial clean sand (FC<10%) deposit, which extends to a depth of at least 20 m at the Shirley site. The thick, clean sand layer does include some thin (up to 50-mm thick) interbedded silt seams and some fine to medium gravel at some depths. The stress-normalized equivalent clean sand tip resistance (q_{c1Ncs}) of the clean sand layer is 100 to 150 at depth of 3.5 to 9.5 m, which increases to 150 to greater than 200 at deeper elevation. Using the Boulanger & Idriss (2016) CPT-based liquefaction triggering procedure (BI-16), the shallower and younger alluvial fine sand unit from a depth of 3.5 m to a depth of 9.5 m is the critical layer (Figure 2). In addition, this layer contributes the most to the calculated Liquefaction Severity Number

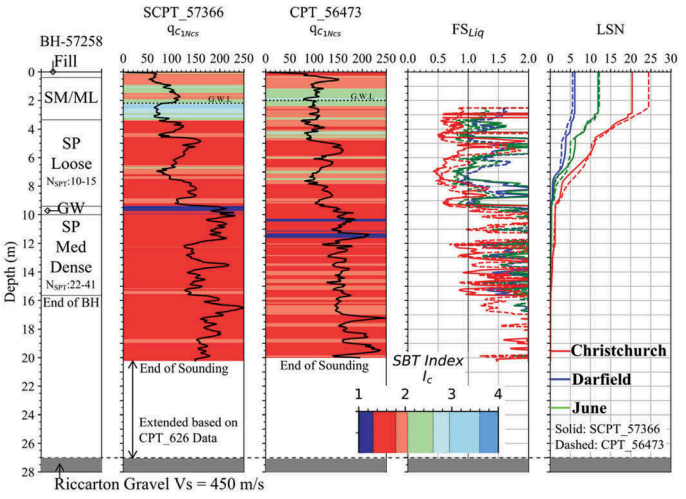

Figure 2. Subsurface characteristics of Shirley site showing the borehole information, CPT-based liquefaction triggering analysis based on BI-16 ($P_L = 50\% \,\&\, C_{FC} = 0.0$) and computed LSN.

(LSN) value. Hence, this layer of sand is most critical to producing liquefaction manifestations at the ground surface. LSN was found to distinguish between sites with and without liquefaction manifestations (van Ballegooy et al. 2014) because it weighs more heavily shallow liquefaction. In our study we found that sand ejecta is likely to occur for a thick clean sand site if LSN exceeds 10. The details of this part of our study will be published separately due to page limitations of this paper.

2.3 *Engineering properties of soil*

SCPT-57366, and CPT-56473 points are used to estimate the engineering properties of the soil units until the end of their soundings (i.e. about 20 m deep). CPT-626 data at the nearby SHLC strong motion station is used to extend the soil profile until the top of the dense Riccarton gravel unit. Figure 3 summarizes the available data and its interpretation using available empirical relationships. The most important parameters for the effective stress analyses are relative density (D_R), shear wave velocity (V_s), and hydraulic conductivity (k). The empirical relationship used to estimate these parameters are summarized in Table 1. The Shirley site profile is subdivided into 6 major layers above the Riccarton gravel as shown in Figure 3. The values and variations of k and D_R govern primarily the results of these simulations which intend to capture hydro-mechanical interaction. The first layer (SM/ML) is treated as silt deposit with lower k relative to the underlying clean fine sand layers SP-2 and SP-3 with a range of higher values (10^{-3} to 10^{-2} cm/s) and relative densities between 30% and 70%. The lower SP-3 and SP-4 clean sand layers have similar values of hydraulic conductivity with relative densities between 40% and 60%. The CL layer is a 2-m thick firm clay layer, which lies atop the dense Riccarton gravel.

2.4 *Input ground motions*

Nearby recorded outcropping rock or downhole ground motions are not available for the CES events. Recorded surface motion at stiff soil sites that exhibit relatively linear site response are used instead to deconvolve top of Riccarton Gravel motions. Markham et al. (2016) produced a suite of deconvolved motions for sites in Christchurch for the major events of the CES. Bradley (2013) is used to determine the amplitude scaling factor at the Shirley site following the procedure used by Luque & Bray (2017). This study employed the fault normal

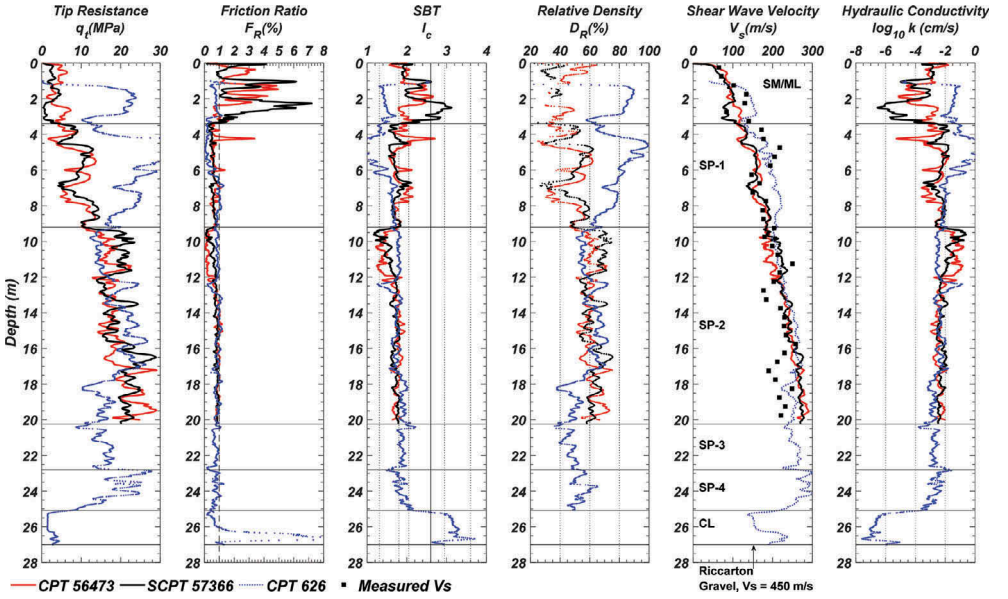

Figure 3. Interpreted soil engineering properties used for FEA.

Table 1. Summary of model parameters used in the numerical simulation

Parameter	SM/ML	SP-1	SP-2	SP-3	SP-4	CL	Ref
Soil Model	PM4Silt	PM4Sand	PM4Sand	PM4Sand	PM4Sand	PIMY	-
Thickness (m)	3.4	5.8	11.0	2.6	2.3	1.9	-
γ (kN/m^3)	17.3–18.3	17.8–19.3	18.6-19.8	19.3	19.3	18.5	RC(15)
I_c	1.9-2.9	1.6-2.1	1.2-1.9	1.7-1.9	1.7-2.0	3.0-3.7	R(09)
q_{c1Ncs}	25-110	75-150	120-200	100-140	130-200	-	BI(16)
D_R (%)	N/A	30-60	55-70	40-50	50-60	-	CPT
S_u (kPa)	50	-	-	-	-	80-100	CPT
V_s (m/s)	100	115-195	170-290	230-260	260-300	150-200	Mc(15)
k_v (cm/s)	10^{-5}-10^{-4}	10^{-3}-10^{-2}	10^{-3}-10^{-2}	10^{-3}-10^{-2}	10^{-3}-10^{-2}	10^{-7}-10^{-6}	RC(15)
# of elements	7	13	22	5	5	4	
PM4Sand (other parameters are set to default as proposed by BZ-17)							
h_{po}	-	0.8	1.0	1.5	1.5	-	Calibrated
n_b	-	1.4	1.4	1.4	1.4	-	T(15)
R	-	1.0	1.0	1.0	1.0	-	M(15)
PM4Silt (other parameters are set to default as proposed by BZ-18)							
h_{po}	10.0	-	-	-	-	-	Assumed

The Idriss and Boulanger (2008), Kulhawy and Mayne (1990), and Jamiolkowski et al. (2001) correlations with weights of 0.4, 0.3, and 0.3, respectively are used to estimate D_R. References are designated as: RC(15): Robertson & Cabal (2015), Mc(15): McGann et al (2015), BZ-17: Boulanger & Ziotopolou (2017), BZ-18: Boulanger & Ziotopolou (2018), T(15): Taylor (2015), and M(15): Markham (2015)

'outcropping' motion resulted from deconvolution analysis using surface motion recorded at Riccarton High School (RHSC) strong motion station. The June 2011 event are two M_w 5.6 and M_w 6.0 separated by 80 minutes. For the purpose of this work, it is analyzed as one stronger event (M_w 6.2) to consider the influence of previous smaller event in generating excess pore water pressure. Figure 4 shows the calculated within motion, which is calculated at the top of the Riccarton Gravel unit.

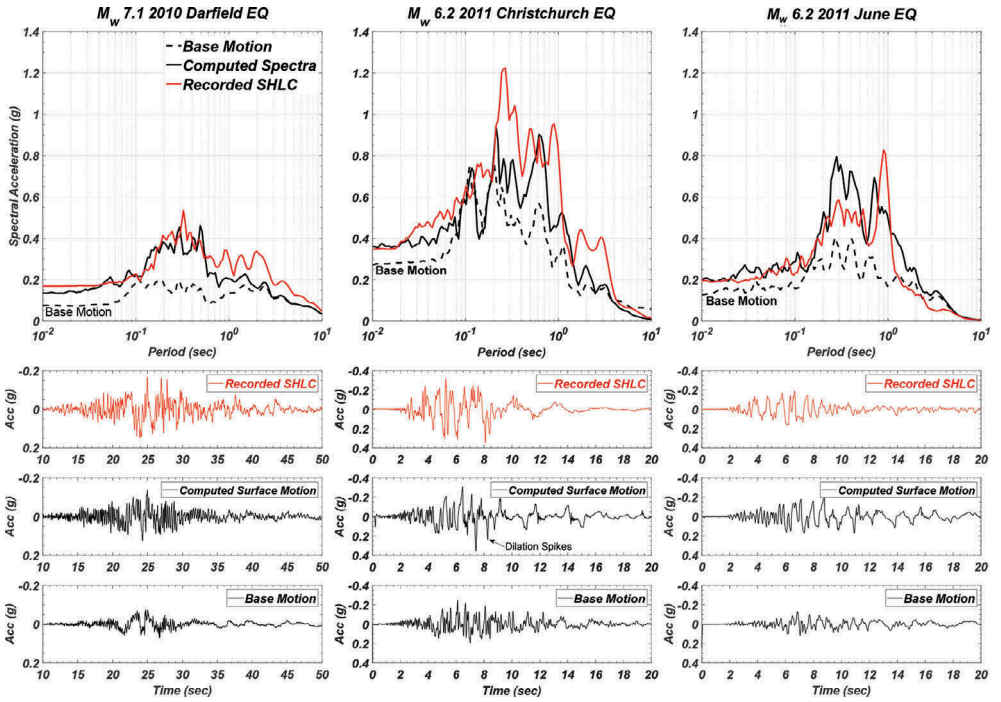

Figure 4. Comparison of acceleration time history and 5% damped acceleration response spectra of recorded instrumentation at SHLC and numerical simulation result at the Shirley site for each CES event.

3 EFFECTIVE STRESS ANALYSIS

3.1 *Finite element model*

The 1D ESA is performed using the open-source finite element analysis (FEA) program OpenSees v3.0 (*http://opensees.berkeley.edu*) with an implicit solver. The analyses employ 2D fully-coupled quad u-p element based on Biot's theory of porous media. The 4-node quad mixed u-p element with reduced integration technique and stabilized single point (SSP) with hourglass control (McGann et al. 2012) is used. The element solves the hydro-mechanical governing equation and compute the nodal displacement and pore pressure based on Zienkiewicz & Shiomi (1984) u-p formulation. With the SSP procedure, the resulting element provide a free volumetric and shear locking element with faster analysis time compared to full integration type of element.

The horizontal movement of each nodes at the same elevation is attached to move together to better represent a 1D simple shear mechanism. To accommodate the compliance of a linear elastic base, the Lysmer & Kuhlemeyer (1969) dashpot is used at the base of the model to apply the shear stress-time history following procedure proposed by Joyner & Chen (1975). The analysis involved 56 of the 4-node SSP quad elements stacked vertically with the number of elements of each soil layer listed in Table 1. The height of each element for each layer is set to be 0.5 m so that it can propagate motion with frequency lower than the 10 Hz maximum frequency content of the within motion. Full Rayleigh damping formulation is implemented in the analysis to construct the damping matrix with damping ratio of 2% at natural frequency (1.84 Hz) and at the fifth modal frequency of the soil deposit (9.2 Hz). The time-step selected for the analysis is 10^{-3} second and checked to ensure it fulfills the CFL condition. The GWL for the simulation is 2.5 m.

3.2 *Constitutive model*

The PM4Sand and PM4Silt constitutive models (Boulanger and Ziotopoulou 2017, 2018) are implemented in OpenSees by Chen et al. (2018). These bounding surface plasticity/critical state models are used to capture the dynamic response of the clean sand and silt layers. User-defined parameters for the models are defined in Table 1. The h_{po} parameter for PM4Sand model is calibrated to give CRR at $N_{c\text{-}Liq}$=15 to be within the range of 15%-85% CRR value based on Boulanger & Idriss (2016). For the saturated silt layer, h_{po} is set to 10.0 based on simple shear element simulations using OpenSees. All secondary parameters not shown are set to default values.

4 SEISMIC SITE RESPONSE

The capability of 1D-ESA to capture the hydro-mechanical response of the Shirley site during earthquake shaking is examined. The aspects of the problem that governed this phenomenon are the generation of excess pore water pressure by the soil models, the resulting change of soil stiffness during earthquake excitation due to the reduction of effective stress, and the hydraulic conductivity of the soil layers which govern the flow of water and redistribution of pore water pressures. Accordingly, the simulation should capture key features of site response in liquefied sites such as dilation spikes due to temporary increase of stiffness as the soil transform from contractive to dilative behavior. It should also capture the lengthening of the site's natural period due to loss of stiffness of the site, which will lead to amplification of spectral acceleration at high periods. The flow of water during and after strong shaking should be also captured.

Figure 4 summarizes the computed surface acceleration-time histories and the 5%-damped acceleration response spectra during the CES events. For the Darfield event, the stiffness of the soil system did not degrade significantly so that the natural period is relatively unchanged and no liquefaction is expected. The computed time history has frequency content similar to the base motion. The spectral acceleration is amplified across most periods of motion as commonly observed when there is little soil nonlinearity. The shapes of the computed spectra and acceleration-time history at the surface are similar to the recorded motion at SHLC where there is no evidence of liquefaction during Darfield earthquake (Wotherspoon et al. 2014). There are reasonable differences because the upper part of the Shirley site differs from that of the SHLC site (Figure 3) and the input motion is the deconvolved motion from RHSC.

The Shirley site experienced significant nonlinearity during the Christchurch event as indicated by the computed surface acceleration-time history that shows dilation spikes followed by long period motion after strong shaking as typically recorded at liquefied sites (Kramer et al. 2011). The amplification of the spectral values at periods lower than 0.1 seconds is caused by the dilation spikes. The site did not amplify the spectra at period of 0.1 to 0.3 seconds. However, for the periods greater than 0.3 seconds, amplification is seen, which indicates a significant decrease of soil stiffness due to liquefaction. Similar observations are noted for the June 2011 event. The SHLC station site experienced liquefaction during the 2011 February Christchurch earthquake (Gingery et al. 2015). Thus, the response spectra shown in Figure 4b are comparable for this event. The response spectra in Figure 4c differ slightly as liquefaction was not observed at the SHLC site for the June 2011 event.

Figure 5 presented computed hydro-mechanical response showing the temporary increase of stiffness which produces the dilation spikes and generation of pore pressure modeled by different soil model. The cyclic shear strain generated during the Christchurch and June 2011 events concentrates at SP-1 layer due to the relatively high generation of excess pore pressure in this layer, which reduces the effective confining stress and shear stiffness. The distribution of the total head better represents the hydraulic conditions during the event, which in turn helps discern the likelihood of vertical water flow as the result of the dissipation process after strong shaking. The Christchurch earthquake generated higher total head difference than the June and Darfield events (as shown in Figure 6). The maximum total head difference from within the SP-1 layer to the groundwater table during Darfield, Christchurch, and June events

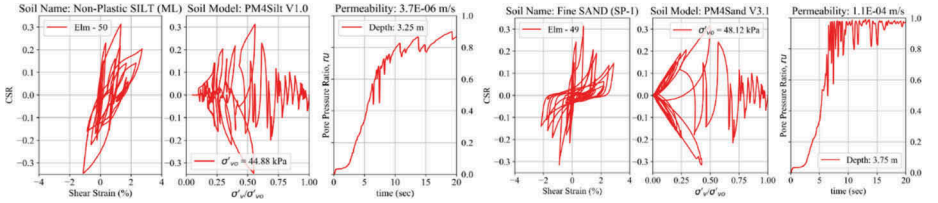

Figure 5. Computed hydro-mechanical response of two elements at different elevations with PM4Silt and PM4Sand) for M_w6.2 22 February 2011 Christchurch event.

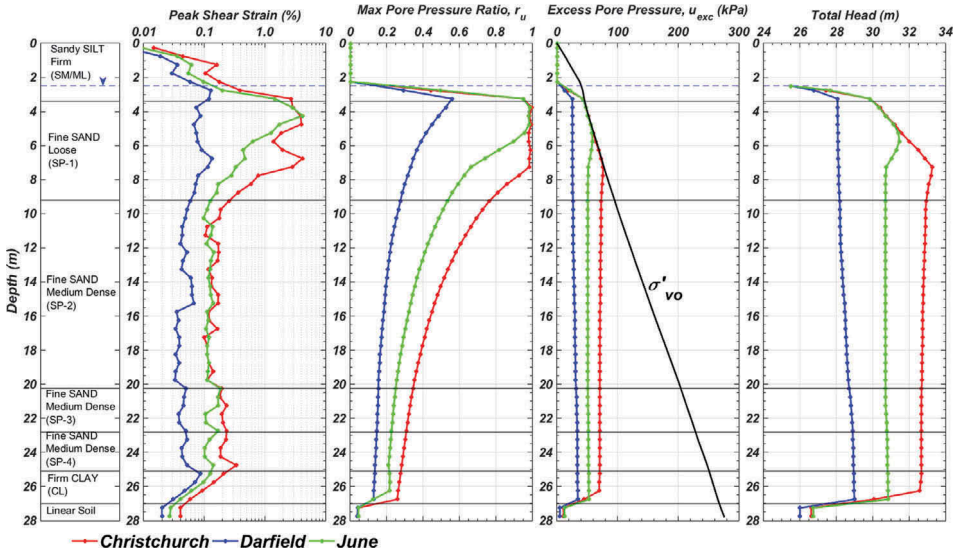

Figure 6. Computed seismic responses of Shirley site for each CES events. Datum elevation is at 28.0 m.

is 2.5 m, 7.5 m, and 6.0 m, respectively with the datum elevation positioned at the bottom of finite element model (28.0 m). The hydraulic gradients computed from the elevation of the maximum computed total head within the SP-1 layer to the GWL elevation for the three earthquake events are 0.23, 1.53, and 1.27. This is equivalent to the difference in water pressures in this 1D simulation with only vertical flow. It is a proxy of the magnitude of total unbalanced energy that must be dissipated to reach an equilibrium state.

The dissipation process induces vertical water flow towards the ground surface that brings soil from the liquefied layer to be ejected at the ground surface. Its theoretical driving mechanism as postulated by Housner (1958) is the magnitude of excess pore water pressure, which is better represented in the general case by hydraulic gradient to quantify the unbalanced energy and the direction of water flow. The computed hydraulic gradient can differentiate the different amounts of ejecta observed at the Shirley site after the three different earthquakes. The greater the hydraulic gradient, which is caused by more intense shaking, the more likely the induced-vertical water pressure will cause more severe surface manifestations of liquefaction. The greater supply of water from the medium dense fine sand (SP-2) unit below SP-1 also enhances the formation of ejecta for the Christchurch event.

5 CONCLUSION

Dynamic finite element effective stress analysis is performed to back-analyze a well-investigated free-field liquefiable site at the Shirley Intermediate School during the 2010-2011

Canterbury earthquake sequence. The Shirley site profile contains a thick alluvial clean sand deposit, which governs its seismic site response and performance. The simulation results show reasonable agreement with the recorded motions at the nearby SHLC station which also did not liquefy during the Darfield event but did liquefy during the Christchurch event. In terms of the site's hydro-mechanical response, 1D-ESA captures the fundamental mechanics of soil liquefaction triggering and post-liquefaction soil response as shown in the computed surface motion, element behavior, and acceleration response spectra. Importantly, the differing hydraulic regimes calculated by the analyses for three earthquake events help explain the different amounts of ejecta observed at the Shirley site. The computed hydraulic gradient from the maximum total head in the liquefiable layer to the GWL elevation quantifies the total unbalanced energy in the form of vertical water flow which produces ejecta. The observed trends in the analytical results suggest this approach may serve as the basis for developing an alternative approach for estimating the severity of the surface manifestations of liquefaction.

ACKNOWLEDGEMENT

The authors acknowledge support from the Ministry of Finance of Republic of Indonesia through Indonesia Endowment Fund for Education (LPDP) for the first author. This study was also funded by the Pacific Earthquake Engineering Research (PEER) Center through the Transportation Systems Research Program (TSRP) and by the National Science Foundation (NSF) under Grant CMMI-1561932. All opinions, findings, and conclusions or recommendations expressed in this material are those of the authors and do not necessarily reflect the views of the NSF. Data compiled by New Zealand and U.S. researchers following the CES events, which is now available in the New Zealand Geotechnical Database and GEER reports, are essential to this research. Data and insights shared by Dr. Sjoerd van Ballegooy of Tonkin + Taylor, Ltd. were also of great help. Discussions with Long Chen and Prof. Pedro Arduino of the Univ. of Washington regarding the implementation of PM4Sand and PM4Silt in OpenSees were of great value.

REFERENCES

Ambraseys, N. & Sarma, S. 1969. Liquefaction of soils induced by Earthquake. *Bull. Seismol. Soc. Am*. V. 59(2), 651–664.

Boulanger, R. W. & Idriss, I.M. 2016. CPT-based liquefaction triggering procedure. *ASCE J. Geotech. Geoenviron. Eng*. V.142(2).04015065.

Boulanger, R. W., & Ziotopoulou, K. 2017. PM4Sand (version 3.1): A sand plasticity model for earthquake engineering applications. *Report No. UCD/CGM-17/01*. 112 pp

Boulanger, R. W., & Ziotopoulou, K. 2018. PM4Silt (Version 1): A silt plasticity model for earthquake engineering applications. *Report No. UCD/CGM-18/01*.

Bradley, B.A. 2013. A New Zealand-specific pseudospectral acceleration GMPE for active shallow crustal earthquakes based on foreign models. *Bull. Seismol. Soc. Am*. V 103(3). 1801–1822.

Bray, J., Cubrinovski, M., Zupan, J., & Taylor, M. 2014. Liquefaction effects on buildings in the central business district of Christchurch. *Earthquake Spectra* 30(1). 85–109.

Chen, L & Arduino, P. 2018. Implementation of PM4Sand in Opensees. *PEER Report*, UC Berkeley.

Gingery, J., Elgamal, A., & Bray, J.D. (2015). Response spectra at liquefaction sites during shallow crustal earthquake. *Earthquake Spectra* 31(4). 2325–2349

Housner, G.W. 1958. The mechanism of sandblows. *Bull. Seismol. Soc. Am*. Vol. 48 pp. 155–161.

Idriss, I, & Boulanger, R. 2008. Soil Liquefaction During Earthquakes. (EERI), MNO-12; 2008.

Ishihara, K., 1985. Stability of natural deposits during earthquakes. In: *Proceedings of the 11th ICSMFE. San Francisco, CA, USA*, 1, pp. 321–3376.

Jamiolkowski, M., LoPresti, D.C.F., & Manassero, M. 2001. Evaluation of relative density and shear strength of sands from CPT and Flat DMT. *SBSGC (GSP 119) ASCE, Reston*, VA, 201–2238.

Joyner, W. B., & Chen, A. T. F. 1975. Calculation of nonlinear ground response in earthquakes. *Bull. Seismol. Soc. Am*. 65 (5),1315–1336.

Kulhawy, F.H. & Mayne, P.H. 1990. Manual on estimating soil properties for foundation design. *Electric Power Research Institute*. August 1990.

Luque, R., & J. Bray. 2017. Dynamic analyses of two buildings founded on liquefiable soils during the Canterbury EQ sequence. *ASCE J. Geotech. Geoenviron. Eng*. 143 (9): 04017067.

Lysmer, J. M., & Kuhlemeyer, R. L. 1969. Finite-dynamic model for infinite media. *J. Engrg. Mech. Div*. 95(4), 859–877.

Markham, C., Bray, J. D., Macedo, J., & Luque, R. 2016. Evaluating nonlinear effective stress site response analyses using records from the CES. *Soil Dynamics & Earthquake Eng*. 82, 84–898.

McGann, C., Bradley, B., Taylor, M., Wotherspoon, L., & Cubrinovski, M. 2015. Development of an empirical correlation for predicting shear wave velocity of Christchurch soils from cone penetration test data. *Soil Dynamics & Earthquake Eng*. 75, 66–675

McGann, C. R., Arduino, P., & Mackenzie-Helnwein, P. 2012. Stabilized single-point 4-node quadrilateral element for dynamic analysis of fluid saturated porous media. *Acta Geotechnica* 7(4). 297–311.

Robertson, P.K., 2009a. Interpretation of cone penetration tests – a unified approach. *Can. Geotech. J*. 46:1337–1355

Robertson, P. K., & Cabal, K. L. 2015. Guide to cone penetration testing for geotechnical engineering, 6th Ed., Gregg Drilling & Testing, Inc. Signal Hill, CA.

Taylor, M. 2015. The geotechnical characterization of Christchurch sands for advanced soil modelling. *Ph.D. dissertation, Univ. of Canterbury*. Christchurch, New Zealand.

van Ballegooy S, Malan P, Lacrosse V, Jacka ME, Cubrinovski M, Bray JD, O'Rourke TD, Crawford SA, & Cowan H. 2014. Assessment of liquefaction-induced land damage for residential Christchurch. *Earthquake Spectra*. 30(1):31–55.

Wotherspoon, L.M., Orense, R.P., Bradley, B.A., Cox, B.R., Wood, C.M. & Green, R.A. 2014. Geotechnical characterization of Christchurch strong motion stations. Eq.Comm.Rep. Project No. 12/629; v 2.

Zienkiewicz, O.C. & Shiomi, T. 1984. Dynamic behavior of saturated porous media; the generalized Biot formulation and its numerical solution. *Int. J for Numerical Methods in Geomechanics*. 8. 71–96.